Analyst

Accepted Manuscript

ROYAL SOCIETY OF CHEMISTRY

www.rsc.org/analyst

Cite this: DOI: 10.1039/c0xx00000x

www.rsc.org/xxxxxx

ARTICLE TYPE

Highly specific detection of thrombin by an aptamer-based suspension array and the interaction analysis via microscale thermophoresis

Yanan Liu[a], Nan Liu[b,*], Xinhua Ma[b], Xiaoli Li[b], Jia Ma[a,b], Ya Li[b], Zhijiang Zhou[a,*], Zhixian Gao[a,b,*]

Received (in XXX, XXX) Xth XXXXXXXXX 20XX, Accepted Xth XXXXXXXXX 20XX

DOI: 10.1039/b000000x

A novel aptamer-based suspension array detection platform was designed for the sensitive, specific and rapid detection of human α-thrombin as a model. Thrombin was firstly recognized by a 29-mer biotinylated thrombin-binding aptamer (TBA) in solution. Another 15-mer TBA modified magnetic beads (MBs) captured the former TBA-thrombin to form an aptamer–thrombin–aptamer sandwich complex. The median fluorescent intensity obtained via suspension array technology was positively correlated with thrombin concentration. The interactions between TBAs and thrombin were analyzed using microscale thermophoresis (MST). The dissociation constants could be respectively achieved to be 44.2 ± 1.36 nM (TBA1-thrombin) and 15.5 ± 0.637 nM (TBA2-thrombin), which demonstrated the high affinities of TBAs-thrombin and greatly coincided with previous reports. Interaction conditions such as temperature, reaction time, and coupling protocol were optimized. The dynamic quantitative working range of the aptamer-based suspension array was 18.37-554.31 nM, and the coefficients of determination R^2 were greater than 0.9975. The lowest detection limit of thrombin was 5.4 nM. This method was highly specific for thrombin without being affected by other analogs and interfering proteins. The recoveries of thrombin spiked in diluted human serum were in 82.6-114.2%. This innovative aptamer-based suspension array detection platform not only exhibits good sensitivity based on MBs facilitating highly efficient separation and amplification, but also suggests high specificity by the selective aptamers binding, thereby suggesting the expansive application prospect in research and clinical fields.

1. Introduction

Suspension array technology, which was first exploited by Luminex Corporation as early as 1997, provides an aqueous phase environment for macromolecular or bio-molecular interaction. The whole suspension array system includes laser detector, plate handling platform, sheath fluid delivery system, high-speed digital signal processor, and the core component-color-coded beads. Different color-coded beads can be distinguished by changing the ratio of the two dyes, allowing the modification of different probe molecules, nucleic acid or protein.[1] Final signal responses are observed using red and green laser lights for identifying each bead and fluorescent reporter molecules captured on its surface. As an open platform, this technology has been widely used for the detection of a variety of targets, such as bacteria,[2] mycotoxin,[3] virus,[4] cytokines,[5] pollutants,[6] and so on. Furthermore, there are numerous advantages for quantitative bio-analysis, such as simple operability, flexibility, high sensitivity, and time-saving.[7-9]

Except the detection technology itself, the recognition component is also essential for the detection of target. In recent years, antibodies have been gradually replaced by aptamers. Aptamers are short single-stranded oligonucleotides, RNA or DNA,[10] with low molecular weight and simple structure, that can be obtained by the systematic evolution of ligands by exponential enrichment.[11] It can selectively bind to various target molecules with high affinities and easy to be synthetized with low-costing compared with antibody. [12,13] Moreover, it folds adaptively to form specific 3D space structures, including hairpin, pseudoknot, bulge, and G-quartet, which facilitate tight coupling with the target.[14,15]Their target molecules cover small molecules, proteins, nucleic acids, cells, or microorganisms,etc.[16] Herein, we integrate specific aptamer and advanced suspension array technology to establish a sensitive and rapid detection platform. The platform can be applied in various fields based on different types of aptamer. We would demonstrate the sensitivity, specificity and time-saving of the platform via the detection of the typical mode target- thrombin.

Thrombin is an important serine protease that exhibits both procoagulant and anticoagulant functions in human blood coagulation.[17-19] The quantitative detection of thrombin is very crucial in early diagnosis, curative effect monitoring and prognosis judgment for hematological systemic disorders. Two DNA aptamers with 15-mer (denoted as TBA1 in this article) and 29-mer (denoted as TBA2 in this article) have been specifically selected against thrombin corresponding to its two electropositive exosites, namely fibrinogen and heparin sites, situated on the sides of the active site.[20-25] Recently, based on the molecular interaction, many selective and sensitive aptamer-based methods have been developed, such as electrochemical and electrochemiluminescence assays[26], however which require complicated electrode modification and multistep washing processes; and gold nanoparticle-based assays[27] which may not be suitable for high-throughput screening and large-scale clinical examination.

In the present work, the novel aptamer-based suspension array detection platform was designed to determine human α-thrombin by a sandwich format (TBA1–thrombin–TBA2). Aptamer-modified carboxylic magnetic beads (MBs) in our platform facilitate the easy separation of target from solution or blood

serum. Through the double recognition with TBA2 and the probe bead, thrombin was quantitatively determined via simple coupling processes. The platform not only exhibits its unique superiorities in the respect of sensitivity, specificity, low background interference, time-efficiency and good repeatability, but also suggests the potential in drug screening and large-scale clinical examination.

In addition, the analysis and verification of the binding affinity between protein and its aptamer is also crucial in the fundamental studies and drug screening. We introduced a novel biophysical approach-microscale thermophoresis (MST) to analyze the aptamers-thrombin interaction by obtaining series of fluorescence-time curves at concentration gradients of thrombin in capillaries. It's an ultrasensitive and convenient technology based on the directed movement of the fluorescence labeled molecule in a temperature gradient with low-volume fluidics, called thermophoresis, which was related to numerous molecular properties such as size, charge, hydration shell or conformation.[27-32] Moreover, MST doesn't need surface immobilization and high sample consumption as same as the isothermal titration calorimetry or surface plasmon resonance.[32] And the determination of binding affinity could be completed in about 10 min in free solution. In this study, it suggested MST was an appropriate approach for biomolecular interaction and the results coincided with the proposed protocol in the aptamer-suspension array platform.

2. Experimental

2.1. Chemicals and materials

Carboxylic MB was purchased from Luminex Corp (Austin, TX, USA). Human α-thrombin was obtained from Enzyme Research Laboratories (South Bend, IN, USA). Streptavidin R-Phycoerythrin conjugate (SA-PE; 1mg mL^{-1}) was supplied by Invitrogen Corp (Carlsbad, CA, USA) and freshly diluted 100 times before use. 1-Ethyl-3-[3-dimethylaminopropyl] carbodiimide hydrochloride (EDC) was purchased from J&K Chemical Co., Ltd. (Beijing, China). Amino and carbochain-modified TBA1 and biotinylated TBA2 with respective sequences of 5′-NH_2-$(CH_2)_6$-T_{10}-GGTTGGTGTGGTTGG-3′ and 5′-Biotin-T_5-AGTCCGTGGTAGGGCAGGTTGGGGTGACT-3′, fluorescence labelled TBA1 and TBA2 with the sequences of 5′-FAM-T_{10}-GGTTGGTGTGGTTGG-3′ and 5′-FAM-T_5-AGTCCGTGGTAGGGCAGGTTGGGGTGACT-3′ were synthesized by Sangon Biotechnology Co., Ltd. (Shanghai, China). Human IgG and silver staining kit were obtained from Boster Bioengineering Co., Ltd. (Wuhan, China). Trypsin and chymotrypsin were purchased from Yaxin Biotechnology Co., Ltd. (Shanghai, China). Bovine serum albumin (BSA), ovalbumin (OVA), and human serum were obtained from Amresco (Solon, OH, USA), Sigma–Aldrich (Saint Louis, MO, USA), and Chengwen Immune Chemical Laboratory (Beijing, China), respectively. Pageruler-prestained protein ladder was obtained from Thermo Scientific (USA).

2-(N-Morpholino) ethanesulfonic acid (MES) buffer (0.1 M, pH= 4.5), 0.1% (w/v) sodium dodecyl sulfate (SDS) buffer, 100× Tris–EDTA buffer (TE buffer, pH= 8.0), 0.02% (w/v) Tween-20 buffer, blocking buffer [phosphate-buffered saline (PBS, 0.01 M, pH= 7.4) containing 1% BSA], binding buffer [Tris–HCl (pH= 7.4) containing 20 mM Tris, 1 mM $MgCl_2$,1 mM $CaCl_2$, 140 mM NaCl and 5 mM KCl], washing buffer [Tris–HCl (pH= 7.4) containing 20 mM Tris, 1 mM $MgCl_2$, 1 mM $CaCl_2$, 140 mM NaCl, 5 mM KCl, and 0.02% Tween-20], DNA oligonucleotides dissolving buffer [PBS (pH= 7.4) and 1 mM $MgCl_2$], and thrombin storage buffer (50 mM sodium citrate, 0.2 M NaCl and 0.1% PEG-8000, pH=6.5), selection buffer for the measurement of the binding affinity [Tris–HCl (pH= 7.4) containing 20 mM Tris, 1 mM $MgCl_2$, 1 mM $CaCl_2$, 140 mM NaCl, 5 mM KCl, and 0.1% Tween-20] were prepared in our laboratory. All buffers used were prepared with the ultra-purified water and filtered with 0.45 μm filters. The water used throughout the experiment was purified by the Milli-Q system (Millipore, Bedford, MA, USA), which had a minimum resistivity of 18 MΩ•cm.

2.2. Apparatus

A CS-1000 Autoplex Analyzer system (Perkin-Elmer Inc., USA) including *x*PONENT™ 3.0 software based on Luminex *x*MAP® technology (Luminex Corp, Austin, TX, USA) was employed for laser beaming, fluorescent signal capture, analysis, and data processing. Thermo-shaker (ST70-2, Nanjing Huchuan Electronics Co. Ltd., China) with temperature control was employed to incubate coupling assays in microtiter plates at medium speed (800 rpm). A 96-well magnetic separator from our laboratory was used to separate MBs from the solution in 96-well microtiter plates (No. 3789 Costars, Corning, Milpitas, CA, USA) throughout all the tests by the suspension array system. The superficial morphology of the MBs were observed by scanning electron microscopy (SEM, LEO 1530VP, Germany). A hemocytometer (Qiujing Biochemical Reagent and Instrument Co., Ltd., Shanghai, China) was employed to count the beads in solution by using an optical microscopy (CX22, Olympus Co. Ltd., Japan). The binding affinities between aptamers and thrombin were calculated by microscale thermophoresis (Monolith NT.115, Munich, Germany).

2.3. Preparation of probe beads

TBA1 was coupled on the MBs as the probe beads by the following procedure. Firstly, the blank carboxylic MB suspension was sonicated for 30 s and resuspended. Prior to use, TBA1 was denatured at 95 °C for 5 min and then slowly cooled down to room temperature (RT) to obtain a proper folding structure. A 100 μL aliquot (approximately 1.25×10^6 beads) of the bead suspension was transfered into a centrifuge tube coated with a tin foil paper to avoid from light exposure and rinsed with 100 μL of MES buffer. The MBs in the tube was separated for 5 min by a magnetic separator and the supernatant was removed. Secondly, the beads were resuspended in 8.5 μL of MES by vortex, in which 4 μL of TBA1 (100 μM in dissolving buffer) was injected and then 2.5 μL of 10 mg mL^{-1} fresh EDC was added. The coupling reaction was proceeded by vortex at 800 rpm for 4 h at RT in the dark. The coupled beads were repeatedly washed with

0.02% Tween-20. Thirdly, the residual carboxyl sites on the beads' surface were blocked by a blocking buffer on the shaker for another 20 min of vortex after discarding the supernatant. The washing steps were repeated thrice by 0.1% SDS. Afterward, the probe beads were resuspended in 100 μL of TE buffer.

The number of probe beads was counted using the hemocytometer under an optical microscope. After counting, the beads were diluted to 2000 beads per microliter in TE. Finally, the probe beads were stored in the dark at 4 °C.

2.4. Optimization of coupling protocol, incubation time and temperature

To form a sandwich complex between thrombin and TBAs, TBA2 was added after denaturing at 95 °C for 5 min under two different protocols depicted in Scheme 1. Protocol 1 presents the routine injected sequence. Specifically, 1 μL of the probe bead set was added in one well of a 96-well plate in the dark. After adding of 10 μL of thrombin (0.9 μM in storage buffer) and the binding buffer to keep the total volume to 50 μL per well, the mixture was incubated by vortex at 800 rpm for 30 min at 37 °C to facilitate thrombin capture by the probe beads. The beads were then separated using a magnetic separator and rinsed by a washing buffer. TBA2 was injected and incubated in a binding buffer at the above conditions for the sandwich coupling. Subsequently, the mixture was separated and washed again. Finally, the sandwich complexes with 50 μL of SA-PE injected was incubated at the same conditions. The obtained median fluorescent intensity (MFI) was automatically determined by utilizing the suspension array system and collected using the *x*PONENT™ 3.0 software. The addition sequence of TBA2 was adjusted in protocol 2. Briefly, thrombin was incubated with TBA2; and the probe beads were then injected into the complex with incubation to form the sandwich compound completely. Through separating and washing processes, 50 μL of SA-PE was added and incubated at the above conditions. The subsequent analysis was performed using the suspension array system.

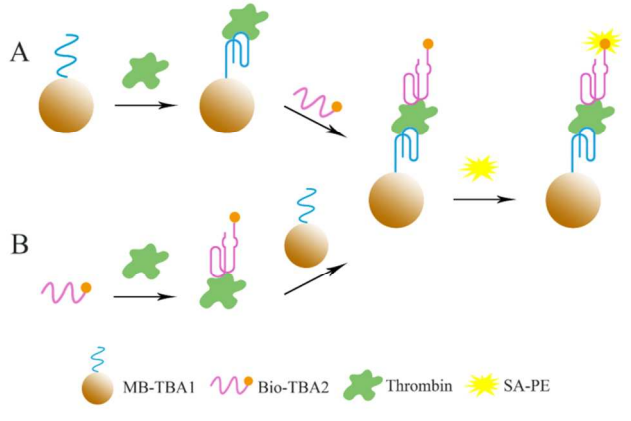

Scheme 1 Two different protocols for the recognition between MB–TBA1, thrombin and bio-TBA2. (A) Protocol 1. (B) Protocol 2. The condition of each incubation process was same, namely vortex at 800 rpm for 30 min at 37 °C. After the recognition for thrombin, TBAs form specific space structures.

The incubation time was set to 30 min and 1 h according to our pre-experiment to choose the preferable one under protocol 2. The optimal incubation temperature was chosen among 25, 32, and 37 °C, which were generally adopted in biological experiments.

2.5. Assay for the detection of thrombin

We tested nine concentration gradients of thrombin (7, 14, 28, 56, 90, 112.5, 225, 450, and 900 nM within a volume of 10 μL) and acquired a set of MFI values. Thrombin sample and 9 pmol of TBA2 mixed with 2000 probe beads per well. The reaction processes were carried out according to protocol 2 at the optimum incubation condition. After deducting the background value, i.e., the blank, the ratios of all MFI values obtained by the concentration gradients of thrombin to the positive control (MFI_0) were achieved. The standard curves were then plotted.

2.6. Specificity test

To test the specificity of the aptamer in recognizing of thrombin, we analyzed thrombin, its analogs and the interfering proteins, such as trypsin, chymotrypsin, BSA, OVA and human IgG, by performing the following procedure. A mixture of 10 μL of thrombin, 10 μL of protein, 9 pmol of TBA2, and the binding buffer was incubated by vortex at 800 rpm for 30 min at 25 °C. The probe beads were added into the mixture with subsequent incubation at the same conditions for 30 min. The MBs were then separated to eliminate uncoupled substances and rinsed with the washing buffer. The final MFI values were measured by suspension arrays.

2.7. Recovery test in human serum

To access the applicability of the assay in complex biological samples, diluted human serum without thrombin, which was tested before, was used as a sample matrix to evaluate the recovery in the assay. The spiked thrombin (28, 56, 112.5, 225, 450, and 900 nM) in the 100-fold diluted human serum with 10 μL per sample was detected by suspension arrays.

2.8. Characterizing the surfaces of MBs by SEM

The superficial morphologies of MBs at different reaction stages, such as the uncoupled MBs, the probe beads, and the MBs in sandwich structure, as well as the morphologies after the entire reaction chain, were observed via SEM.

2.9. The determination of binding affinity and biomolecular interaction analysis using MST

The fluorescence labelled TBA1 and TBA2 was dissolved in the selection buffer with a constant concentration of 100 nM. Before the MST experiment, all reagents containing the buffer and thrombin and so on were centrifuged at 14,000 ×*g* for 10 min to remove impurities. The serial dilution of thrombin (2250, 1125,

562.5, 281.25, 140.63, 70.31, 35.16, 17.58, 8.79, 4.39, 2.20, 1.10, 0.55, 0.27 and 0.14 nM) mixed with the isometric fluorescence labelled aptamer were investigated in capillaries by MST.

3. Results and discussion

3.1. Optimization of coupling protocol and conditions

To obtain relatively high fluorescent intensities, the coupling protocol and conditions required to be optimized. In this assay, 100 beads were counted and recognized by suspension array system in a well. All the fluorescent intensity values on the surface of the 100 beads within one sample didn't present a Gaussian distribution but a skewness of distribution. So the MFI was used to obtain the results which also were the default value of suspension array system when making a normal testing. And the detection of 96 samples could be completed within 15 min by suspension array itself.

Two TBAs that can bind to two exosites of thrombin were employed in the aptamer-based suspension array tests to form the sandwich format. One was immobilized onto the beads to capture thrombin, and the other labelled with biotin was used to detect the thrombin. Daniel et al,[33] reported that TBA1 can bind to both of the exosites of thrombin with different affinities, whereas TBA2 can only recognize the heparin binding site. Considering the above-mentioned recognition characteristic and the relatively weaker affinity of TBA1 to thrombin compared with that of TBA2,[25,33-35] we designed two protocols to obtain higher MFI. The binding of TBA1 to the heparin binding site reduced the number of TBA2 binding to thrombin and thus decreased the sensitivity in the assay. Therefore, we changed the adding sequence of TBAs in protocol 2 to obtain the higher binding efficiency between two TBAs and thrombin.

Fig. 1A shows that, both MFIs in the two different protocols increased with the increasing addition volume of TBA2. It suggests the formation of a complete reaction chain. As expected before, the signal of protocol 2 was higher than that of protocol 1. Thus, we considered the protocol 2 as the preferable reaction scheme. The result greatly coincided with previous reports,[33] wherein the highest increase in surface plasmon resonance can be obtained by the same protocol. What's more, the phenomenon for the different selectivity of TBAs toward thrombin exosites may be explained by their secondary structures. TBA1 can form a stable intramolecular G-quadruplex structure binding to thrombin, which adopts a specific space structure like a chair connected by two TT loops and one TGT loop.[36-40] TBA2 comprises of two G-quadruplex structures in which eight guanines participate. These quartet structures of aptamers contribute to the stability of thrombin–aptamer compounds. However, except for the G-quadruplex, TBA2 also can form a small duplex at the dangling ends; this duplex contributes to the exclusive selectivity of the TBA2 to binding heparin site of thrombin.[21]

Fig. 1B showed that the MFIs were slightly higher after 30 min than after 1 h of incubation with 18 and 27 pmol addition of TBA2. As a result, 30 min was considered as the best incubation time

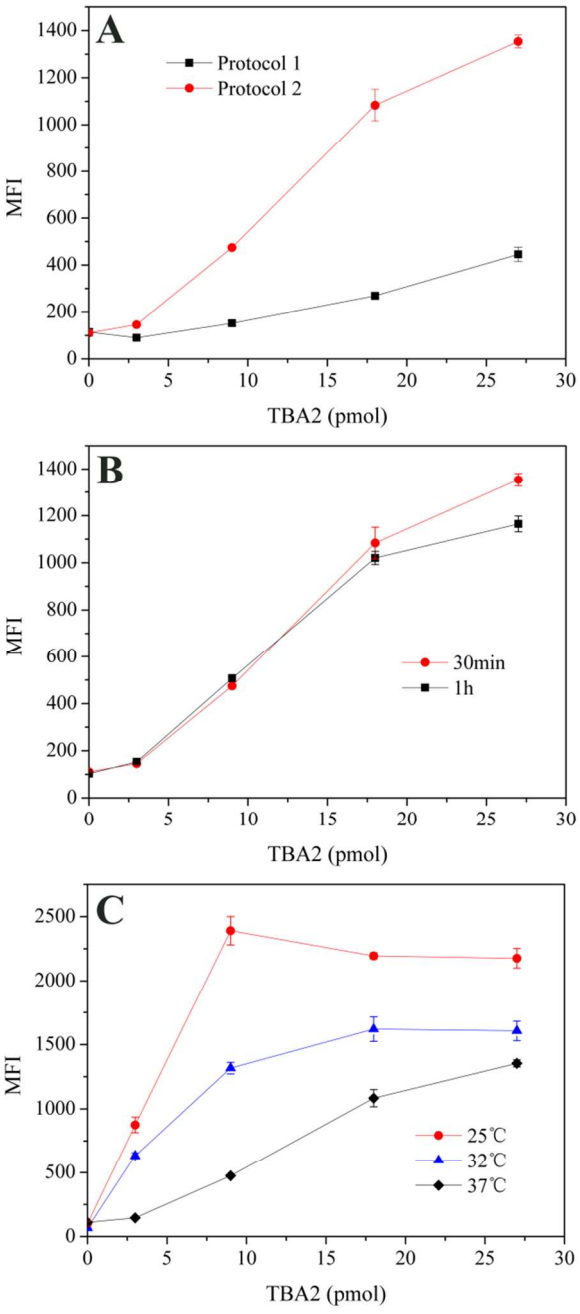

Fig. 1 (A) Optimization of coupling protocol. Two protocols were performed at 37 °C for 30 min. (B) Optimization of incubation time under protocol 2 at 37 °C. (C) Optimization of incubation temperature. The incubation time was conducted to 30 min. Thrombin sample volume was 10 μL, and the addition concentration was 0.9 μM in these assays.

.

In general, 37 °C is the best temperature to keep the activity of most proteins. However, this temperature might not be the optimum for thrombin–TBA binding, and the recognition of TBAs to the binding sites of thrombin does not need the best activity of thrombin. Thus, we set the different temperature to explore the best reaction condition. Fig. 1C showed that the

sandwich assay yielded the highest MFI value at 25 °C with a 9 pmol of TBA2. Herein, we conducted our assays using protocol 2 for 30 min in each incubation step at 25 °C.

3.2. Analytical performance of the aptamer-based suspension array

Gradient concentrations of thrombin (7, 14, 28, 56, 90, 112.5, 225, 450, and 900 nM) were analyzed by suspension arrays under the optimal reaction protocol and conditions to build the standard curve. According to the obtained values of MFI/MFI_0, a four-parameter logistic regression equation and linear equation were employed to fit the data for the detection of thrombin in different working ranges (Fig. 2). These procedures were slightly different from those in our former studies.[41-43] At low thrombin concentrations (< 56 nM), i.e., a small quantity of thrombin–TBA2 compound, thrombin was easily irreversibly captured by the relatively excessive probe beads in the liquid. The reaction probably resembled the ordinary chemical reaction and displayed a linear dose-response relationship. At relatively high thrombin concentrations (> 56 nM), i.e., it might be after the point of inflection, the relationship was illustrated as an ordinary logistic regression standard curve.

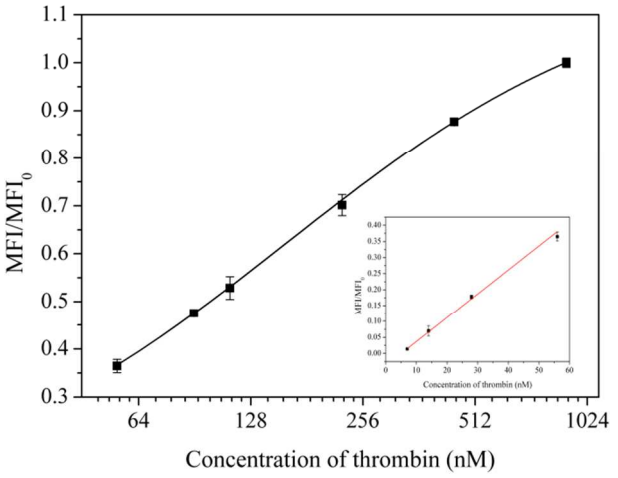

Fig.2 Standard curve for the detection of thrombin.

The logistic regression equation was $y = 1.2099 - 1.1527/(1+x/169.8417)^{0.9056}$ with a determination coefficient (R^2) of 0.9995 and a working range of 56-900 nM. The linear equation was $y = 0.0071x - 0.0304$ (R^2=0.9975) with the working range of 7-56 nM in the inset graph of Fig. 2. The dynamic quantitative detection range was 18.37 nM to 554.31 nM (IC_{10} – IC_{90}), and the lowest detection limit (LDL) was 5.4 nM (three times of the blank standard deviation). It suggests that the aptamer-based suspension array technology is highly sensitive for the detection of thrombin. This platform can be further developed to detect more targets simultaneously. The described technology is more accurate and precise than other technologies, such as gold nanoparticle-based assay (R^2=0.96)[44] and electrochemiluminescence quenching (R^2=0.9886)[39]. Although the LDLs of the former two methods were lower than that of our work, the key materials in their methods, such as fibrinogen-Au nanoparticles, tris (2, 2'-bipyridyl) ruthenium (II) and platinum nanoparticles, were not easy to synthesize and expensive. Compared with these former methods, our method exhibited more predominant merits, such as easier MB procurement, simpler operation, and greater potential for large-scale clinical examination and drug screening.

3.3. Specificity test

Molecular recognition selectivity is important to evaluate the analytical methods and the detection platform. The obtained values of MFI/MFI_0 by adding of structurally related analogs and interfering proteins were shown in Fig. 3. The disruptors, except trypsin, did not obviously interfere in the sandwich aptamer-based suspension array assays at the same concentration relative thrombin. Trypsin of the serine protease family is a strong hydrolyzed protein used for numerous biotechnological processes, such as trypsin proteolysis or trypsinization (http://en.wikipedia.org/wiki/Trypsin). It has a similar amino acid hydrolysis position and amino acid composition to thrombin. To confirm the hydrolysis or interference effect of trypsin, we designed an SDS polyacrylamide gel electrophoresis (SDS-PAGE) assay with single or mixed proteins.

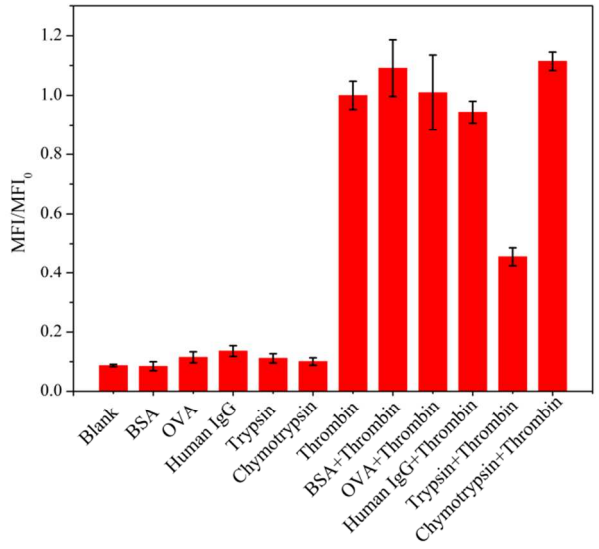

Fig.3 Specificity test for the sandwich assay. The concentration of thrombin and other proteins were 0.9 μM.

Sliver staining was performed to amplify the dyeing effects, and the electrophoregram was presented in Fig. 4. A significant light thrombin stripe was observed in lane 3 compared with the obvious stripe in lane 1. The stripe of trypsin (approximately 24.4 KDa) presented translucence in lane 2 (trypsin) and did not change in lane 3 (trypsin+thrombin). This result confirmed the hydrolysis of thrombin by trypsin and explained the interference in the specificity test caused by trypsin. Trypsin can specifically hydrolyze peptide bonds at the carboxyl side of arginine and lysine residues contained in thrombin. Whereas, the concrete hydrolysis position in thrombin by trypsin would not be discussed in this work. In addition, other proteins such as OVA, human

IgG, and chymotrypsin didn't interact with thrombin. These tests demonstrated the high specificity of the aptamer-based suspension array technology for detecting of thrombin. The hydrolysis of thrombin by trypsin may contribute to the detection and research of acute pancreatitis patients' serum.

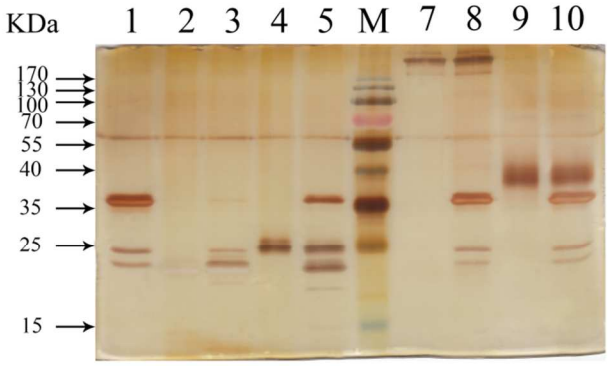

Fig. 4 The electrophoregram via silver stain.
Lane 1: thrombin (~36 KDa); Lane 2: trypsin (~24 KDa); Lane 3: trypsin + thrombin; Lane 4: chymotrypsin (~25 KDa); Lane 5: chymotrypsin + thrombin; Lane 6: marker; Lane 7: human IgG; Lane 8: human IgG + thrombin; Lane 9: OVA (~40 KDa); Lane 10: OVA + thrombin. Before performing the SDS-PAGE, single thrombin and the mixture of thrombin and each other interference with the same volume and concentration were incubated for 30 min at 25 °C.

3.4. Recovery test

Table 1
Detection of thrombin in 100-fold diluted human serum samples (n=3).

Samples	Amount spiked (nM)	Amount measured[a] (nM)	Recovery (%)	RSD (%)
1	28	27.08	96.7	6.1
2	56	48.01	85.7	8.4
3	112.5	102.06	90.7	7.3
4	225	185.84	82.6	9.9
5	450	513.99	114.2	1.9

[a] Mean values of three determinations.

The human serum, which is considered as one of the most complex sample matrixes, was imported in the detection system to test the stability of the established aptamer-based suspension array technology. The results were presented in Table 1. The recovery values of the spiked thrombin were 82.6% to 114.2% with relative standard deviations (RSDs) below 10%. The recovery within the range of 80-120% was considered acceptable for basic scientific research. It proved the feasibility of this establishing platform and indicated that the method has potentials for the quantitative detection of thrombin and designing clinic diagnostic kit in biological samples.

3.5. Characterization of the superficial morphology of MBs using SEM

The key component of suspension array technology is the carboxylated fluorescent coding polystyrene microsphere with different diameters (non-magnetic: 5.6 μm and magnetic: 6.5 μm) carrying many carboxyl sites on the surface to allow biological probe coupling.[45] The superficial morphologies of MBs at different reaction stages were qualitatively observed using SEM (Fig.S1 in Supplementary Data). Fig. S1 (a) displayed the uncoupled MB with a diameter of approximately 6.5 μm and a rough surface making it different from the non-magnetic polystyrene microsphere,[43] which is caused by tiny Fe_3O_4 granules coating on the outermost surface of the polystyrene microparticle. We found the morphology of MB that coupled with TBA1 did not significantly vary except for a very thin layer on the surface demonstrated in Fig. S1 (b). As a relatively small molecule, TBA1 cannot form overlapping layers, which isn't similar to protein coating on the surface of solid carrier. So it did not show an obvious binding state in the MBs. Nevertheless, Fig. S1 (c) displayed a layer of sticky substance on the surface of the probe beads after recognizing thrombin, which resulted in a smooth appearance. This result confirmed that thrombin was bound successfully on the surface of MBs. After coupling with SA-PE, the MB–TBA1–thrombin–TBA2-PE compound was formed, and the sticky substance became thickened [Fig.S1 (d)]. Meanwhile, it demonstrated the formation of the complete reaction chain.

3.6. MST analysis for the thrombin-aptamer interaction

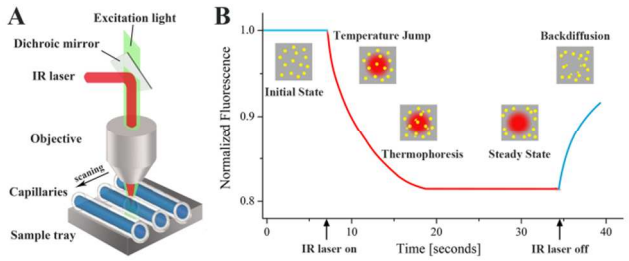

Fig.5 MST setup and thermophoresis assay. (A) Schematic representation of MST optical system. The solution with a total volume of 4 μL in the capillary was locally heated with a diameter of 50 μm by the IR laser. The fluorescence in the solution was excited and collected through the objective. Thermophoresis signal was detected within a temperature gradient induced by the IR laser. (B) The typical MST curve for a capillary. The TBAs, thrombin and TBAs-thrombin complex molecules were homogeneously distributed until the IR laser was turned on. As soon as the IR laser was turned on, a fast temperature-jump (denoted as T-Jump) was observed within less than a second, followed by the thermophoresis of the fluorescence labeled aptamer out of the heated area. When IR laser was turned off, the fluorescence labeled aptamer diffused back.

MST, as an advanced and rapid interaction analysis technology, could monitor the directed movement of the fluorescence molecule labelled on the TBAs in a localized temperature gradient spanning 2-6°C induced by the infrared laser (IR laser, 1480 nm) through an objective (Fig.5A).[28,29] Meanwhile, the

fluorophore labelled on the TBAs in the capillaries were excited and the fluorescence was collected by the same objective. In the MST experiment, more than a dozen of capillaries including a series of concentration gradient of thrombin and constant concentration of the labelled TBA were scanned and detected in sequence. Fig.5B showed a typical MST fluorescence-time curve in a capillary, which represented the variable normalized fluorescence value following with the different IR laser state. Within one of capillaries the mixed solution containing a certain concentration of thrombin and TBA with the constant concentration was homogenous in the initial state. And the constant initial fluorescence was obtained. Since the IR laser was turned on, TBA and thrombin in the solution began to diffuse and then reached a stable state. Similarly, the fluorescence in the heated spot decreased with the movement of the labelled TBA from the heat region to the cold because of the thermophoresis and eventually achieved the equilibrium. In this process, T-Jump was arisen within about 50 ms and primarly relied on the local surroundings of the fluorophores which were affected by the binding of thrombin in nearby. Either the thermophoresis or T-Jump signal could be used to calculate the dissociation constant. Turning off the IR laser resulted in the labelled TBA diffused back and the fluorescence rebounded. And then one typical MST curve at the certain concentration of thrombin and constant labelled TBA was completed and recorded (Figure.5B).[28,30] A series of fluorescence-time curves could be obtained at different concentration gradient of thrombin in the capillaries. Those curves composed to the integrated fluorescence-time traces from unbound to bound status of TBA-thrombin (in Fig.6A).

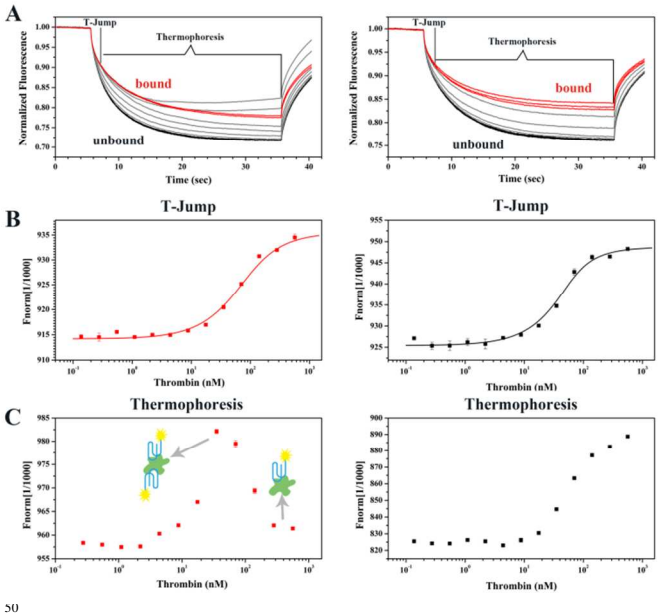

Fig.6 MST experiments for the determination of dissociation constant and binding mode of thrombin with TBA1 (left) and TBA2 (right). (A) MST time traces of titrations of thrombin against TBA1 (left) and TBA2 (right). Traces corresponding to bound and unbound states were colored black and red, as well as partially bound intermediates were shown in gray. (B) T-Jump signals fitted for calculating the dissociation constant of thrombin with TBA1 (left) and TBA2 (right). (C) The dotted line of thermophoresis signals of thrombin against TBA1 (left) and TBA2 (right) for analysis of the binding mode.

MST was employed to verify the high binding affinities between the TBAs and thrombin. In this MST experiment, we applied the T-Jump signal to calculate the dissociation constant and the thermophoresis signal to analyze the interaction stoichiometry. The fluorescence ratio signal F_{norm} was obtained via the equation $F_{norm} = F_{hot} / F_{cold}$ (average fluoresence values in selected areas from the line marked by the blue and red respectively in Fig.5B). The different thrombin concentration resulted in a gradual changing F_{norm}. The change in T-Jump was plotted to yield the binding curve, which could be fitted to derive dissociation constants. The dissociation constant obtained for TBA1-thrombin binding in buffer was 44.2 ± 1.36 nM (left in Fig. 6B), which agreed with the previous report. [34] As shown in the right of Fig.6B, changes in the T-Jump signal stemmed from the TBA2-thrombin binding was fitted to yield a K_d of 15.5 ± 0.637 nM. It could be demonstrated that two aptamers rendered high binding affinities in nM level with thrombin and could be well applied for the detection of thrombin. MST not only allowed for the determination of the binding affinity, but also provided other information about the interaction mechanism.

We also found that the thermophoresis signal could be used to demonstrate the binding mode of TBA1-thrombin (left in Fig. 6C). The right of Fig.6C presented a typical thermophoresis curve of TBA2 bound with thrombin, while the curve of TBA1 bound thrombin with high affinity displayed a different peak, which could not be observed in the T-Jump signals.[28] In the left of Fig.6C, the signal increased with the concentration of thrombin and then reached a peak, whereas decreased again until to an equilibrium, which suggested that different TBA1-thrombin complexes were formed. It was estimated that about two TBA1 molecules combined with one thrombin simultaneously at the peak; and then along with the increased concentration of thrombin, only one TBA1 bound with thrombin finally. This special thermophoresis phenomenon assisted in proving the theory that the TBA1 can combine with both the fibrinogen and heparin binding exosites of thrombin.[33] It also explained the necessity of optimization of the reaction protocols and was able to be employed for further understanding of the TBAs-thrombin molecular interaction.

4. Conclusion

We have developed a sensitive and specific aptamer–based suspension array platform for detecting biomolecules. It was demonstrated that the platform was straightforward and reliable in analyzing the model target-human α-thrombin with simple operation, high sensitivity, and low cost. It could be used for the rapid, accurate, high-efficiency and quantitative determination for thrombin, which demonstrated the practicability of the detection platform. The recovery we obtained in the detection of thrombin spiked in diluted human serum showed the great potentials for practical clinical applications. Concretely, it provides an alternative for the early clinical diagnosis and therapy of diseases in the coagulation system. Additionally, the high affinities between TBA1 or TBA2 and thrombin were testified by the T-Jump signals obtained through the novel MST technology for determining the dissociation constant. The thermophoresis signals yielded by the combination of TBA1-thrombin were employed

for analyzing the binding mode, which verified the optimized protocol in the assay. Furthermore, the detection kit for thrombin based on the platform can be developed and widely applied to a large-scale screening and detection for serum samples. Moreover, the detection for other molecules by this platform using relevant aptamers is being conducted based on the competitive method by our team.

Acknowledgements

The authors gratefully acknowledge the financial supported by the National Natural Science Foundation of China (No.81273078).

References

1 G. Deng, K. Xu, Y. Sun, Y. Chen, T. Zheng, and J. Li, , *Anal. Chem.*, 2013, **85**, 2833-2840.

2 S. H. Maňásková, F. J. Bikker, E. C. I. Veerman, A. van Belkum and W. J. B. van Wamel, *J. Immunol. Methods*, 2013,**397**, 18-27.

3 Y. Wang, B. Ning, Y. Peng, J. Bai, M. Liu, X. Fan, Z. Sun, Z. Lv, C. Zhou, Z. Gao, *Biosens. Bioelectron.*,2013,**41**,391-396.

4 I. A. Hamza, L. Jurzik, M. Wilhelm, *J. Virol. Methods*, 2014,**204**, 65-72.

5 L. Wang, K. D. Cole, A. Peterson, H. He, and A. K. Gaigalas, *J.Proteome Res.*,2007,**6**, 4720-4727.

6 Y. Guo, J. Tian, C. Liang, G. Zhu, W. Gui, *Microchim. Acta*,2013,**180**,387-395.

7 S. L. van Brunschot, J. H. W. Bergervoet, D. E. Pagendam, M. de Weerdt, A. D. W. Geering, A. Drenth, R. A. A. van der Vlugt, *J. Virol. Methods*, 2014,**198**, 86-94.

8 M. A. Makiya, J. A. Herrick, P. Khoury, C. P. Prussin, T. B. Nutman, A. D. Klion, *J. Immunol. Methods.*, 2014,**411**,11-12.

9 A. R. Connolly, R. Palanisamy, M. Trau, *J. Biotechnol.* ,2010,**145**, 17-22.

10 A.D. Ellington, J.W. Szostak, *Nature*, 1990,**346**, 818-822.

11 C. Tuerk, L. Gold, *Science* , 1990,**249**,505-510.

12 S. Tombelli, M. Minunni, M. Mascini, *Biomol. Eng.*, 2007,24, 191-200.

13 P. Sundaram, H. Kurniawan, M. E. Byrne, J. Wower, *Eur. J. Pharm. Sci.*, 2013,**48**, 259-271.

14 D. M. Tasset, M. F. Kubik, W. Steiner, *J. Mol. Biol.*, 1997,**272**,688-698.

15 F. Radom, P. M. Jurek, M. P. Mazurek, J. Otlewski, F. Jelen, *Biotechnol. Adv.*, 2013,**31**, 1260-1274.

16 T. Smuc, I. Y. Ahn, H. Ulrich, *J. Pharm. Biomed. Anal.*, 2013,**81-82**,210-217.

17 K. G. Mann, K. Brummel, S. Butenas, *J. Thromb. Haemo.* ,2003,**1**, 1504-1514.

18 D. Musumeci, D. Montesarchio, *Pharm. Ther.*, 2012,**136**, 202-215.

19 Q. Zhao, X. Wang, *Biosens. Bioelectron.* ,2012,**34**,232-237.

20 G. Zhou, X. Huang, Y. Qu, *Biochem. Eng. J.*, 2010,**52**, 117-122.

21 P. H. Lin, R. H. Chen, C. H. Lee, Y. Chang, C. S. Chen, W. Y. Chen, *Colloids Surf. B*, 2011,**88**,552-558.

22 X. Wang, Q. Zhao, *Microchim. Acta.*, 2012,**178**, 349-355.

23 I. V. Gribkova, V. A. Spiridonova, A. S. Gorbatenko, S. S. Denisov, F. I. Ataullakhanov, E. I. Sinauridze, *Blood Coagulation & Fibrinolysis*, 2014,**25** ,39-45.

24 Q. Yue, T. Shen, L. Wang, S. Xu, H. Li, Q. Xue, Y. Zhang, X. Gu, S. Zhang, J. Liu, *Biosens. Bioelectron.* ,2014,**56**, 231-236.

25 I. R. Olmsted, Y. Xiao, M. Cho, A. T. Csordas, J. H. Sheehan, J. Meiler, H. T. Soh, D. J. Bornhop, *Anal. Chem.*, 2011,**83**,8867-8870.

26 L. Deng, Y. Du, J. J. Xu, H. Y. Chen, *Biosens. Bioelectron.*, 2014,**59**, 58-63.

27 B. Li, Y. Wang, H. Wei, S. Dong, *Biosens. Bioelectron.*, 2008, **23**,965-970.

28 M. Jerabek-Willemsena, T. André, R. Wanner, H. M. Roth, S. Duhr, P. Baaske, D. Breitsprecher, *J. Mol. Struc.*, 2014,**1077**,101-113.

29 P. Baaske, C. J. Wienken, P. Reineck, S.Duhr, D. Braun, *Angew. Chem. Int. Ed.*, 2010, **49**, 1-5.

30 C. J. Wienken, P. Baaske, U.Rothbauer, D.Braun, S.Duhr, *Nat. Commun.* 2010.

31 Y. Mao, L.Yu, R. Yang, L. Qu, P. de B. Harrington, *Talanta*, 2015, **132**, 894-901.

32 M. Jerabek-Willemsen, C.J. Wienken, D. Braun, P. Baaske, S. Duhr, *Assay Drug Dev. Techn.* , 2011, **9**, 342-353.

33 C. Daniel, F. Melaine, Y. Roupioz, T. Livache, A. Buhot, *Biosens. Bioelectron.*, 2013,**40**,186-192.

34 L. C. Bock, L. C. Griffin, J. A. Latham, E. H. Vermaas, J. J. Toole, *Nature*, 1992,**355**,564-566.

35 Q. Zhao, M. Wu, X. Chris Le, X.F. Li, *Trends Anal. Chem.*, 2012,**41**,46-57.

36 K. Padmanabhan, K. P. Padmanabhan, J. D. Ferrara, J. E. Sadler, A. Tulinsky, *J. Biol.Chem.* ,1993,**268**,17651-17654.

37 R. F. Macaya, P. Schultze, F. W. Smith, J. A. Roe, J. Feigon, *Biochemistry* , 1993,**90**,3745-3749.

38 M. Fialova, J. Kypr, M. Vorlickova, *Biochem. Biophys. Res. Commun.*, 2006, **344**,50-54.

39 Y. Liao, R. Yua, Y. Chai, L. Mao, Y. Zhuo, Y. Yuan, L. Bai, S. Yuan, *Sens. Actuators B-Chem.*, 2011, **158**,393-399.

40 S. Niu, L. Qu, Q. Zhang, J. Lin, *Anal. Biochem.*, 2012,**421**,362-367.

41 N. Liu, P. Su, Z. Gao, M. Zhu, Z. Yang, X. Pan, Y. Fang, F. Chao, *Anal. Chim. Acta.*, 2009,**632**,128-134.

42 N. Liu, Z. Gao, H. Ma, P. Su, X. Ma, X. Li, G. Ou, *Biosens. Bioelectron.*, 2013,**41**,710-716.

43 N. Liu, W. Liang, X. Ma, X. Li, B. Ning, C. Cheng, G. Ou, B. Wang, J. Zhang, Z. Gao, *Biosens. Bioelectron.*, 2013, **47**,92-98.

44 C. K. Chen, C. C. Huang, H. T. Chang, *Biosens. Bioelectron.*, 2010,**25**,1992-1927.

45 Z. Sun, Y. Peng, M. Zhang, K. Wang, J. Bai, X. Li, B. Ning, Z. Gao, *Food Control*,2014,**40**, 300-309.

[a]*School of Chemical Engineering and Technology, Tianjin University, Tianjin, 300072, P. R. China*

[b]*Tianjin Key Laboratory of Risk Assessment and Control Technology for Environment and Food Safety, Tianjin Institute of Health and Environmental Medicine, Tianjin 300050, P. R. China*

E-mail address*: LNQ555@126.com (N. Liu), zzj@tju.edu.cn (Z. Zhou), gaozhx@163.com (Z. Gao). Tel: +86 22 84655060*

† Electronic Supplementary Information (ESI) available: [details of any supplementary information available should be included here]. See DOI: 10.1039/b000000x/